Aquatic Toxicology 268 (2024) 106843

Contents lists available at ScienceDirect

Aquatic Toxicology

journal homepage: www.elsevier.com/locate/aqtox

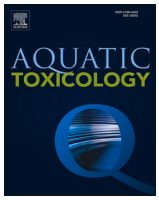

Exposure and recovery: The effect of different dilution factors of treated and untreated metal mining effluent on freshwater biofilm function and structure

Lidia Vendrell-Puigmitja *, Lluís Bertrans-Tubau, Maria Roca-Ayats, Laia Llenas, Lorenzo Proia, Meritxell Abril

BETA Tech Center, TECNIO Network, University of Vic-Central University of Catalonia, Ctra de Roda 70, 08500 Vic, Spain

ARTICLE INFO

Keywords:
Metal mining effluents
Aquatic biofilm
Exposure and recovery
Artificial streams
Dilution capacity

ABSTRACT

Abandoned mines generate effluents rich in heavy metals, and these contaminants are released uncontrolled into the nearby aquatic ecosystems, causing severe pollution. However, no real solution exists, leaving a legacy of global pollution. In this study, the efficiency of the treatment technologies in reducing the ecological impacts of mining effluents to freshwater ecosystems with different dilution capacities was tested using biofilm communities as biological indicators. The functional and structural recovery capacity of biofilm communities after 21 days of exposure was assessed. With this aim, we sampled aquatic biofilms from a pristine stream and exposed them to treated (T) and untreated (U) metal mining effluent from Frongoch abandoned mine (Mid Wales, UK). Additionally, we simulated two different flow conditions for the receiving stream: high dilution (HD) and low dilution (LD). After exposure, the artificial streams were filled with artificial water for 14 days to assess the biofilm recovery. Unexposed biofilm served as control for biofilm responses (functional and structural) measured throughout time. During the exposure, short term effects on biofilm functioning (photosynthetic efficiency, nutrient uptake) were observed in T-LD, U-HD, and U-LD, whereas long term effects (community composition, chl-a, and diatom metrics) were observed on the structure of all biofilms exposed to the treated and untreated mining effluent. On the other hand, metal accumulation occurred in biofilms exposed to the mining effluents. However, a functional recovery was observed for all treatments, except in the U-LD in which biofilm structure did not present a significant recovery after the exposure period. The results presented here highlight the need to consider the dilution capacity of the receiving stream to assess the real efficiency of treatment technologies applied to mining effluents to mitigate the ecological impact on freshwater ecosystems.

1. Introduction

Metal effluents generated during mining activities are sources of water pollution that can arise while the mine is active but, without remedial action, this pollution source can persist long after the mining operation ceases (Younger et al., 2004; Byrne et al., 2012; Kossoff et al., 2014). When mines are abandoned, mining effluents are discharged uncontrollably into the surrounding aquatic ecosystems. These unsupervised discharges from abandoned mines are an important source of pollution in several river catchments around Europe (Younger et al., 2004; Skousen et al., 2019).

In mining effluents, heavy metals are often dissolved in the water and can be easily absorbed or uptaken by aquatic organisms. This can lead to a bioaccumulative fate and biomagnification of the metal throughout the trophic network (Younger et al., 2003; Häder et al., 2020; Chand and Vanavana, 2022). Aquatic biofilms, as primary producers, are at the bottom of the trophic food chain in freshwater ecosystems, being the starting point for bioaccumulation and transfer of heavy metals to higher trophic levels (Bere et al., 2012; Leguay et al., 2016; Hong et al., 2020). In addition, metal pollution could lead to metabolic, functional, and structural alterations in aquatic biofilms (Corcoll et al., 2011; Vendrell-Puigmitja et al., 2020), with different ecological implications at ecosystem level (Morin and Coste, 2006; Wu, 2016). Biofilms contribute to the overall river ecosystem functioning through key ecosystem functions such as nutrient cycling, or primary production (Allan and Castillo, 2007; Battin et al., 2016; Kaplan et al., 1987) and they can rapidly integrate the environmental changes, making them valuable ecological indicators (Romaní et al., 2013).

* Corresponding author.

https://doi.org/10.1016/j.aquatox.2024.106843
Received 13 August 2023; Received in revised form 15 January 2024; Accepted 19 January 2024
Available online 20 January 2024

To reduce the impact of mining effluents on freshwater ecosystems, different treatment processes such as chemical precipitation, chemical oxidation, ion exchange, nanofiltration, reverse osmosis, electrocoagulation and electrodialysis are used nowadays to treat metal mining effluents before discharging them into the receiving stream (Tripathi and Ranjan, 2015). In this context, the LIFE DEMINE project (LIFE16 ENV/ES/000,218) developed an innovative treatment process that combines electrocoagulation and nanofiltration processes. Nanofiltration combines small pore size (nanometre range, MWCO < 2000 Da) and charge to selectively remove divalent cations from solution while allowing monovalent ions to permeate (Mohammad et al., 2015). Electrocoagulation applies an electric current to destabilize and coagulate suspended particles, including heavy metals, facilitating their removal from the water (Moussa et al., 2017). This technology was tested in Frongoch abandoned metal mine (Gwynedd, Wales - 52°21′02.8″N 3°52′31.5″W) that exploited lead (Pb) and zinc (Zn) for nearly 200 years, discharging mining effluents uncontrollably to the Afon Ysywyth catchment ever since (Mullinger 2004; Edwards et al., 2016).

In a stream affected by a mining effluent, aside from the mining effluent load and heavy metals bioavailability (Park et al., 2011), the polluting effect can be modulated also by the stream flow and its dilution capacity (Tchounwou et al., 2012). Therefore, when a mining effluent is treated, the overall reduction in the ecological impact caused by the mining effluent will be determined not only by the efficiency of the selected treatment technology, but also by the dilution capacity of the receiving stream (Tchounwou et al., 2012).

Although the toxic effects of heavy metals in freshwater communities, including biofilms, have been widely described (Guasch et al., 2002; A. Serra, 2009; Corcoll et al., 2011; Wu, 2016; Vendrell-Puigmitja et al., 2020), very few studies have addressed the effects of a real and complex metal mining effluent on them, especially considering different dilution capacities of the receiving stream. Additionally, the recovery capacity of aquatic biofilm communities after the exposure to a pollution source such as mining effluents has been poorly studied (Bonnineau et al., 2011; Lambert et al., 2012; Arini et al., 2012b; Bonet et al., 2013 and 2014; Pandey and Bergey, 2018), although interest in recovery behaviour and community resilience in aquatic systems has increased in recent years (Bonnineau et al., 2021). This growing interest comes from the increasing concern, especially through environmental policies such as the European Water Framework Directive (2000/60/EC), about the restoration of chemically contaminated aquatic ecosystems. In fact, during periods of exposure to pollutants, the community composition of aquatic organisms' changes, and the loss of ecological resilience can occur, with long-term implications for ecosystem recovery (Clements et al., 2010).

This research assessed the efficiency of a treatment technology in decreasing the ecological impact of mining effluents on freshwater ecosystems considering different dilution capacities of the receiving stream and using the aquatic biofilm as ecological indicator. The treated effluent generated in Frongoch abandoned mine after the application of a treatment technology developed in the framework of the LIFE DEMINE project was used to perform the present study.

In the present document, we specifically focused on the following questions: (i) What are the ecological effects caused by the treated and untreated mining effluent on the aquatic biofilm structure and functioning under different simulated stream dilution capacities? (ii) Are these communities able to recover their previous functions and structure when returning to pre-disturbance conditions? And iii) Do the treatment technologies decrease the overall ecological impact caused by the mining effluent?

2. Materials and methods

2.1. Experiment design

The experiment was conducted under controlled conditions, using an indoor artificial streams facility that consists of eighteen independent recirculating Perspex channels (0.50 m long x 0.12 m wide). These artificial channels were designed to maintain the water column at 0.02 m depth. Water input at the head of each channel unit was provided from a 5 L carboy using a water pump (EDEN 105, Eden Water Paradise, Italy) connected with silicone tubes. The system was supplied with artificial water (prepared in the laboratory to simulate a pristine stream) as described by Ylla et al. (2009) at 16 °C (Table 1). The water in the carboys was renewed every two days to prevent nutrient depletion during the whole experiment (Fig. 1). Light-emitting diodes (SMD 5730 - 72) were used to provide natural light at an intensity of 110 μmol photons m^{-2} s^{-1}, following a 12 h/12 h light and dark cycle. The bottom of each channel was covered with 35 sandblasted tile glasses of different sizes (1 × 1 cm, 3 × 3 cm, and 11 × 18 cm) as artificial substrate to promote biofilm settlement. Benthic biofilm was achieved by introducing aliquots of a natural biofilm suspension obtained from a pristine stream (Riera Major, Natural Park of Montseny, NE Spain) at each water renewal (every two days) during the colonisation period that lasted 21 days (t21d).

The experiment included the three following temporal periods: colonisation (21 days), exposure (21 days) and recovery (14 days), and biofilm communities of each artificial stream were sampled at different times during each period (see Fig. 1). After the colonisation period, the exposure to the different treatments started. The experiment comprised five treatments that represented a control treatment (maintained with artificial water during all the experiment), the treated (T; 0.8 mg L^{-1} of Zn, and no detected Pb and Cd) and untreated (U; 95, 8.6, and 0.7 mg L^{-1} of Zn, Pb and Cd, respectively) metal mining effluent from Frongoch mining effluent, under two different simulated flow conditions in the receiving stream, obtaining a high dilution (HD) and low dilution (LD) treatment conditions. The exposure was set to mimic the realistic conditions where the treated and untreated mining effluent (with a flow of 0.001 m^3 s^{-1}) discharges to the receiving stream when the lowest (0.005 m^3 s^{-1}) and average (0.055 m^3 s^{-1}) flow historically registered occur. The reference flow conditions were obtained from historical data (2004–2019) from the Frongoch stream provided by Natural Resources of Wales, the Welsh national natural environment agency. Each treatment was performed in triplicates. The dilution factors applied in our experiment to simulate HD and LD conditions mimicked the real dilution occurring when the metal mining effluent from Frongoch abandoned mine reached Frongoch stream under average or low flow conditions. During the exposure and recovery periods, artificial water, and the mining effluents (in the exposure period) were used to mimic the different dilutions and was renewed at each channel every two days.

2.2. Water physico-chemical parameters

Water physico-chemical parameters of each artificial stream were monitored at every water renewal during the whole experiment. Dissolved oxygen concentration (mg·L^{-1}) and saturation (%), temperature (°C), pH, and conductivity (S·m^{-1}) were measured using a portable sensor probe (YSI professional plus, YSI Incorporated, USA). Simultaneously, triplicate water samples of six different artificial streams at each water renewal during the colonisation period, and for each artificial stream during the exposure and recovery periods, were collected and filtered through a 0.22 μm pore glass microfiber filter (Prat Dumas Filter Paper, Couze-St-Front, France) to analyse NO_3^- (APHA, 1992b), NH_4^+ (Reardon et al., 1966) Soluble Reactive Phosphorus (SRP; Murphy and Riley, 1962) and metals. Metal concentrations in water (Zinc (Zn), Lead (Pb) and Cadmium (Cd)) were analysed using flame atomic absorption spectroscopy (AAS, model AA240FS, Varian, USA). Water

Table 1
Physico-chemical water variables measured in the artificial channels during the colonisation ($n = 12$), exposure ($n = 9$), and recovery periods ($n = 6$; Mean ± SD). bdl: below detection limit. DO, dissolved oxygen; T, temperature; SRP, soluble reactive phosphorus; Zn, zinc; Pb, lead; Cd, cadmium. n.a: not available. T-HD: treated high dilution, T-LD: treated low dilution, U-HD: untreated high dilution, U-LD: untreated low dilution. * rm-ANOVA; ** one-way ANOVA. The letters indicate significant differences ($p < 0.05$) between treatments after one-way and rm - ANOVA and Tukey b test.

	DO (mg L^{-1})	Conductivity (µS cm^{-1})	T (°C)	pH	N-NO_3^- (mg L^{-1})	N—NH_4^+ (mg L^{-1})	SRP (mg L^{-1})	Zn (mg L^{-1})	Pb (mg L^{-1})	Cd (mg L^{-1})
Colonisation	9.53 (±0.04)	136 (±4.10)	15.8 (±0.17)	7.06 (±0.01)	0.36 (±0.05)	0.39 (±0.04)	0.12 (±0.00)	n.a	n.a	n.a
Exposure										
Control	9.64 (±0.58)	120 ^{a} (±6.32)	15.7 (±0.40)	6.96 ^{a} (±0.16)	0.38 ^{a} (±0.05)	0.30 ^{a} (±0.02)	0.11 (±0.01)	bdl	bdl	bdl
T-HD	9.52 (±0.52)	124 ^{b} (±4.43)	15.8 (±0.35)	6.96 ^{a} (±0.16)	0.39 ^{a} (±0.04)	0.32 ^{a,b} (±0.02)	0.11 (±0.01)	0.19 ^{a} (±0.01)	bdl	bdl
U-HD	9.41 (±0.46)	130 ^{c} (±3.64)	15.9 (±0.38)	6.72 ^{b} (±0.24)	0.39 ^{a} (±0.04)	0.35 ^{b,c} (±0.03)	0.11 (±0.02)	1.41 ^{b} (±0.06)	bdl	bdl
T-LD	9.49 (±0.48)	225 ^{d} (±12.0)	15.9 (±0.39)	6.69 ^{b} (±0.24)	0.56 ^{b} (±0.06)	0.39 ^{c,d} (±0.02)	0.12 (±0.02)	4.87 ^{c} (±0.25)	bdl	bdl
U-LD	9.47 (±0.40)	225 ^{d} (±10.6)	15.7 (±0.34)	6.29 ^{c} (±0.37)	0.60 ^{c} (±0.07)	0.43 ^{d} (±0.03)	0.10 (±0.01)	21.3 ^{d} (±0.48)	0.17 (±0.06)	0.04 (±0.01)
	n.s *	$F = 393$ $p < 0.001$ *	n.s *	$F = 17.6$ $p < 0.001$ *	$F = 102$ $p < 0.001$ *	$F = 20.6$ $p < 0.001$ *	n.s *	$F = 42.5$ $p < 0.001$ **	n.a	n.a
Recovery										
Control	9.86 (±0.45)	133 ^{a} (±7.09)	15.4 (±0.54)	7.00 (±0.30)	0.36 (±0.03)	0.30 ^{a} (±0.07)	0.11 (±0.01)	bdl	bdl	bdl
T-HD	9.92 (±0.23)	134 ^{a} (±8.75)	16.3 (±0.50)	7.15 (±0.51)	0.36 (±0.03)	0.36 ^{a,b} (±0.03)	0.13 (±0.01)	bdl	bdl	bdl
U-HD	9.95 (±0.20)	134 ^{a} (±7.81)	16.3 (±0.49)	7.11 (±0.11)	0.34 (±0.01)	0.33 ^{a,b} (±0.06)	0.12 (±0.02)	0.18 ^{a} (±0.02)	bdl	bdl
T-LD	9.80 (±0.24)	132 ^{a} (±1.85)	16.3 (±0.55)	7.12 (±0.12)	0.37 (±0.07)	0.34 ^{b,c} (±0.09)	0.13 (±0.01)	0.29 ^{b} (±0.04)	bdl	bdl
U-LD	9.78 (±0.12)	143 ^{b} (±6.14)	16.2 (±0.29)	7.04 (±0.09)	0.37 (±0.05)	0.38 ^{c} (±0.05)	0.12 (±0.01)	0.50 ^{c} (±0.04)	bdl	bdl
	n.s *	$F = 502$ $p = 0.015$ *	n.s *	n.s *	n.s *	$F = 12.2$ $p = 0.001$ *	n.s *	$F = 13.3$ $p < 0.001$ **	n.a	n.a

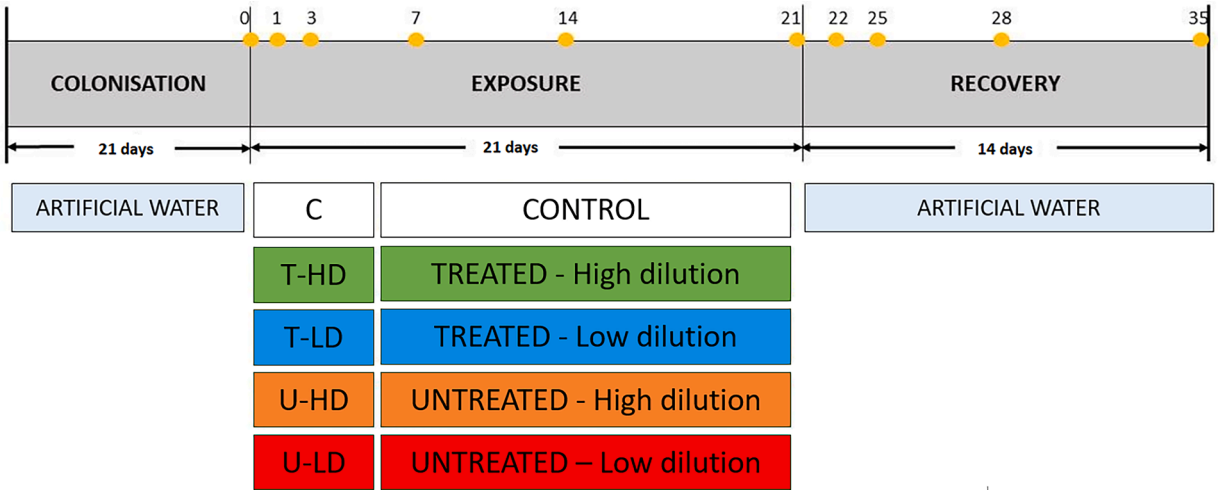

Fig. 1. Experimental design and sampling times (yellow dots, in days) during the exposure (21 days) and recovery (14 days) periods. T-HD: Treated – High dilution, T-LD: Treated – low dilution, U-HD: Untreated - high dilution, and U-LD: Untreated - low dilution.

samples were acidified with nitric acid (HNO_3, ACS, ISO, Panreac) and analysed using an air-acetylene flame and the corresponding hollow cathode lamps. Commercially available AAS standard solutions (TraceCERT, Sigma-Aldrich) were used for the calibrations.

2.3. Biofilm sampling and chl-a

Benthic biofilm was sampled during the exposure (time 0, and after 1, 3, 7, 14 and 21 days) and the recovery period (after 1, 3, 7 and 14 days; Fig. 1). At each sampling day, 3 cm^2 colonized glass tiles were randomly collected from each artificial channel. We measured the photosynthetic efficiency (Yield) and photosynthetic community composition of the biofilm (% relative abundance of each algal group) directly with an amplitude modulated fluorometer (Mini-PAM fluorometer, Walz, Effeltrich, Germany) and a BenthoTorch portable fluorometer probe (bbe Moldaenke, Schwentinenta, DK), respectively. The BenthoTorch spectrally excites algae pigments by three high-frequency-colored LEDs. In response, the algae emit red fluorescent light, and the intensity of this light is used for the calculation of the different types of algae. Then, the biofilm was scraped and suspended in 15 mL of water

from the corresponding stream. The suspension was distributed in aliquots to analyse chlorophyll-a (chl-*a*; Jeffrey and Humphrey, 1975) and then stored at −20 °C for further analysis.

Additionally, at days 0, 7, 14, 21 of the exposure period and days 7 and 14 of the recovery period, we preserved 5 mL of the biofilm suspension by using 5 mL Ethanol 70% to determine the diatom growth rate. The samples were ultrasonicated, and 125 μL of each sample was pipetted onto a Nageotte counting chamber to count the total number of diatom cells following Morin et al. (2010). Data were recorded as cells per sample substrate area (number of cells cm^{-2}). Two distinct types of counting were performed; empty cells considered as 'dead', and cells occupied by chloroplasts considered as 'alive'. According to Guillard (1973), the diatom community growth rates were determined (in cell divisions day^{-1}) by using live diatom counts (expressed in cells mL^{-1}). At day 21 of the exposure and 14 of the recovery periods, we obtained an additional subsample of this biofilm suspension for diatom taxa identification and metal accumulation in the biofilm.

For diatom taxa identification, hydrogen peroxide (30%) was used to remove the organic material and calcium carbonates according to Leira and Sabater (2005). Cleaned frustules were mounted on permanent glass slides using Naphrax (Brunel Microscopes Ltd, UK; RI=1.74). Using standard references and recent nomenclature updates listed in Coste et al. (2009) and Prygiel and Coste (2000), about 400 random frustules per slide were counted at 1,000x magnification, and diatom cells were measured and identified to the lowest taxonomic level feasible.

In order to measure the total metal accumulation in the biofilm, dried biofilm samples from one glass substratum were lyophilized and weighed (g) to determine the dry weight (DW). Then, 200 mg of biofilm DW were digested with 4 mL of concentrated HNO_3 (ACS, ISO, Panreac) and 1 mL of H_2O_2 (30% in water, for analysis, Panreac), brought to 100 mL with ultrapure water (Wasserlab) and stored at 4 °C, as described by Meylan et al. (2003). Total dissolved metals of the digested samples were analysed by flame atomic absorption spectroscopy (AAS, model AA240FS, Varian, USA), using an air-acetylene flame and the corresponding hollow cathode lamps. Commercially available AAS standard solutions (TraceCERT, Sigma-Aldrich) were used for the calibrations.

2.4. Nutrient uptake capacity

The capacity of the biofilm to uptake phosphate and ammonium from the water column during the exposure and recovery periods was measured at each sampling day. Following the methodology described in Vendrell-Puigmitja et al. (2022), we collected a 200 cm^2 glass substrate from each artificial stream and placed it in a 6-L glass aquarium filled with artificial water. The basal nutrient concentration was previously determined, and each aquarium was later spiked with the appropriate volume of Na_2PO_4 (1.42 g L^{-1}) and NH_4^+ (1 g L^{-1}) stock solutions to quadruple the background concentration of both nutrients in the artificial water. Subsequently, we collected water samples (10 mL) from each aquarium at 1, 5, 15, 30, 60, 90, 120, 180, and 240 min after the nutrient addition, and we filtered them through a 0.22 μm glass microfiber filter (Prat Dumas Filter Paper, Couze-St-Front, France) to determine SRP and NH_4^+ concentrations over time and calculate nutrient uptake rates. We calculated the coefficient of the nutrient uptake rate (k, s^{-1}) from the nutrient decay over time as it fitted a negative exponential (or linear) model (Proia et al., 2017).

2.5. Data analysis

The effects of the treatment, dilution, and their interaction on the biofilm response over time during the experiment were determined with data normalised to control (to achieve a standardized data format) using two-way repeated measures ANOVA (tw-rm-ANOVA). Differences among treatments were performed using Tukey-b post hoc test. Differences in physico-chemical parameters between treatments during the colonisation, exposure and recovery periods were evaluated at each water renewal day using one-way ANOVA, as well as metal accumulation on biofilm and diatom metrics. Differences on physico-chemical parameters and diatom metrics over time between treatments were evaluated using one-way repeated measures ANOVA for the exposure and recovery period separately (rm-ANOVA) and using Tukey-b post hoc test. Normality was assessed with the Kolmogorov-Smirnov test and homogeneity of variances with the Bartlett test. All tests were performed using SPSS Statistics software (version 21). To determine differences among treatments on the biofilm community composition (i.e., green algae, cyanobacteria, and diatoms) and the specific diatom species on the biofilm, a one-way ANOSIM was carried out with Bonferroni correction using Past3 version 3.23 for the end of the exposure and the recovery periods. A principal component analysis (PCA) using R Studio software (version 3.6.0) packages FactoMineR (Lê et al., 2008), factoextra (Kassambara, 2016) and ggplot2 (Wickham, 2016) was conducted to visualize the differences among treatments at the end of the exposure (t21d) and recovery (t14d-R) periods, based on both biofilm functional (photosynthetic efficiency and nutrient uptake) and structural (chl-*a*, Margalef Index, diatoms, cyanobacteria, green algae, and Cd, Pb, Zn accumulation) variables. Pearson correlation analysis was performed to explore the relationship between biofilm variables.

The Threshold Indicator Taxa Analysis (TITAN, R package *TITAN2*) was used to classify the response of diatom taxa to significant environmental factors. TITAN is a combination of indicator species analysis and change point analysis (Dufrêne and Legendre, 1997). For each taxon, TITAN seeks an optimum observed change point that maximizes the indicator value (IndVal score) or its standardized IndVal score along a specific environmental gradient. Depending on the relative abundance and occurrence frequency of the taxon on either side of the change point, it is assigned to a negative (vulnerable) or positive (tolerant) response group. The significant environmental factors were selected when a change point or threshold was detected, where there was a synchronous change in the abundance of a number of taxa lying within a narrow range of the predictor variable (Sultana et al., 2020).

3. Results

3.1. Effects of the treatment technology and mine effluent dilutions on water physico-chemical parameters

During the colonisation period, non-significant differences were found in physico-chemical conditions among channels (Table 1 and S2). Water temperature and dissolved oxygen (DO) remained stable throughout the exposure period without differences among treatments (Table 1 and S2). By contrast, pH at T-LD, U-HD and U-LD was significatively lower than in the control (C; Table 1, Tukey b $p < 0.05$). On the other hand, the conductivity was significantly higher at T-LD and U-LD compared to the C (Table 1 and S2, Tukey b $p < 0.05$). Regarding nutrient concentrations in water during the exposure period, soluble reactive phosphorus (SRP) did not differ among treatments (Table 1 and S2) whereas higher ammonium and nitrate concentrations were found at T-LD and U-LD and not in C (Table 1, Tukey b $p < 0.05$). During the recovery period, only U-LD presented higher conductivity than the other treatments, including the C (Table 1, Tukey b $p < 0.05$).

Regarding metal concentrations in water, Cd, Zn and Pb were not detected at t0 (before the beginning of the exposure). Similarly, during the exposure period metals were not detected under C. At t21d, Zn concentration differed among treatments, ranging between 0.19 ± 0.01 in T-HD to 21.3 ± 0.48 mg L^{-1} in U-LD (Table 1 and S2). Pb and Cd were detected only in U-LD (Table 1). Throughout the recovery period, significant differences in Zn concentration were found between treatments T-LD, U-HD, and U-LD compared to the C (87, 79 and 92% higher than C respectively) and among them (Table 1 and S2).

3.2. Effects of the treatment technology and mining effluent dilutions on biofilm structure and function

3.2.1. Photosynthetic efficiency

The photosynthetic efficiency (Y_{eff}) of the biofilm significantly decreased after 24 h of exposure in T-LD, U-HD, and U-LD (Fig. 2-a) compared to the control (C). According to the Y_{eff} results, only the high-dilution scenario (T-HD) did not present significant differences compared to the C. However, under the low dilution conditions (T-LD), the Y_{eff} significantly decreased compared to the C (Table S1). On the contrary, in the untreated effluents (U-HD and U-LD) a significant decrease on the Y_{eff} were observed compared to the C, independently of the dilution factor (Fig. 2-a, Table S1). During the recovery period, the Y_{eff} increased over time, up until the end of the recovery period, without significant differences in Y_{eff} between treatments (Fig. 2-b).

3.2.2. Nutrients uptake

During the exposure period, the soluble reactive phosphorus uptake rate coefficient (k SRP) in T-HD, T-LD and U-HD treatments significantly decreased compared to the C and remained below it (Fig. 3-a, Tukey-b test, $p < 0.05$). Contrarily, U-LD showed a significant increase in k SRP compared to the C during all the exposure period (Fig. 3-a). On the other hand, the NH_4^+ uptake rate coefficient (k NH_4^+) decreased drastically in all treatments compared to the C (Fig. 3- c, Tukey-b test, $p < 0.05$), except for T-HD that remained above the other treatments (30% higher on average; Tukey-b test $p < 0.05$), but still significantly below the C (28% lower on average; Tukey-b test $p < 0.05$). The SRP and NH_4^+ (Table S1) uptake results indicate a significant interaction between treatment and dilution. Additionally, negative correlations were found between Zn accumulation in biofilm and NH_4^+ uptake rate during the exposure period (Pearson's correlation $r = -0.535$, $p = 0.040$).

During the recovery period, the nutrient uptake capacity of the biofilm recovered in all treatments except for the U-LD compared to the C (Fig. 3-b, d). In fact, U-LD nutrient uptake was 53% lower compared to the C by the end of this period. At t14d-R, non-significant differences were found in kSRP between the C and T-HD, and in $k$$NH_4^+$ between the C and T-LD and U-HD (Fig. 3-b, d), which evidenced a significant effect of the dilution and the treatment in the recovery in the nutrient uptake capacity of the biofilm (Table S1).

3.2.3. Chlorophyll- a

The biofilm chlorophyll-a concentration (chl-a) decreased significantly after 24 h of exposure in all treatments compared to the C (Fig. 4-a). Even though chl-a from treated effluents (T) and U-HD recovered over time during the exposure period, at the end of this period, all treatments had chl-a levels below C. The dilution factor did not influence the chl-a concentration in the biofilm exposed to the treated effluents, and non-significant differences were observed between T-HD and T-LD (Fig. 4-a). On the contrary, a significant relation between treatment and dilution in the response of the biofilm exposed to the untreated effluent was observed (U; Table S1), where biomass recovered more under the HD scenario than in the LD scenario.

During the recovery period, the chl-a in all treatments did not recover and remained below the C. Specifically, the U and the T-LD treatments presented the lower chl-a levels highlighting the effect of the dilution and treatment (Fig. 4-b, Table S1).

3.2.4. Biofilm community composition

Regarding the biofilm community composition (counted as units, either single cells or colonies, as appropriate), diatoms dominated the biofilm community just before the beginning of the exposure period, with an average relative abundance of 48.9 ± 3% in all channels (Fig. 5). During the exposure period, the relative abundance of green algae increased in all treatments, being significantly higher than the C in T-LD, U-HD, and U-LD at t21d (one-way ANOSIM $R = 0.186$, $p < 0.001$). At the end of the exposure period (t21d) there was found a significant negative correlation between diatom abundance (based on the main photosynthetic group densities) and Zn concentration (Pearson's correlation $r = -0.695$, $p = 0.004$) and a significant positive correlation between green algae abundance and Zn concentration (Pearson's correlation $r = 0.791$, $p < 0.001$) in biofilm. During the recovery period, biofilm communities were dominated by green algae in all treatments, in a higher proportion than the C (one-way ANOSIM $R = 0.365$, $p < 0.001$)

3.2.5. Diatom metrics

After 21 days of exposure (t21d), a decrease in the diatom growth rate (GR) was observed in biofilm communities exposed to all treatments compared to the C (one-way ANOVA $F = 6.86$, $p < 0.001$; Fig. 6). Eventually, diatom communities under all treatments presented a significant decrease in diatom cells size compared to the C (Figure S1; one-

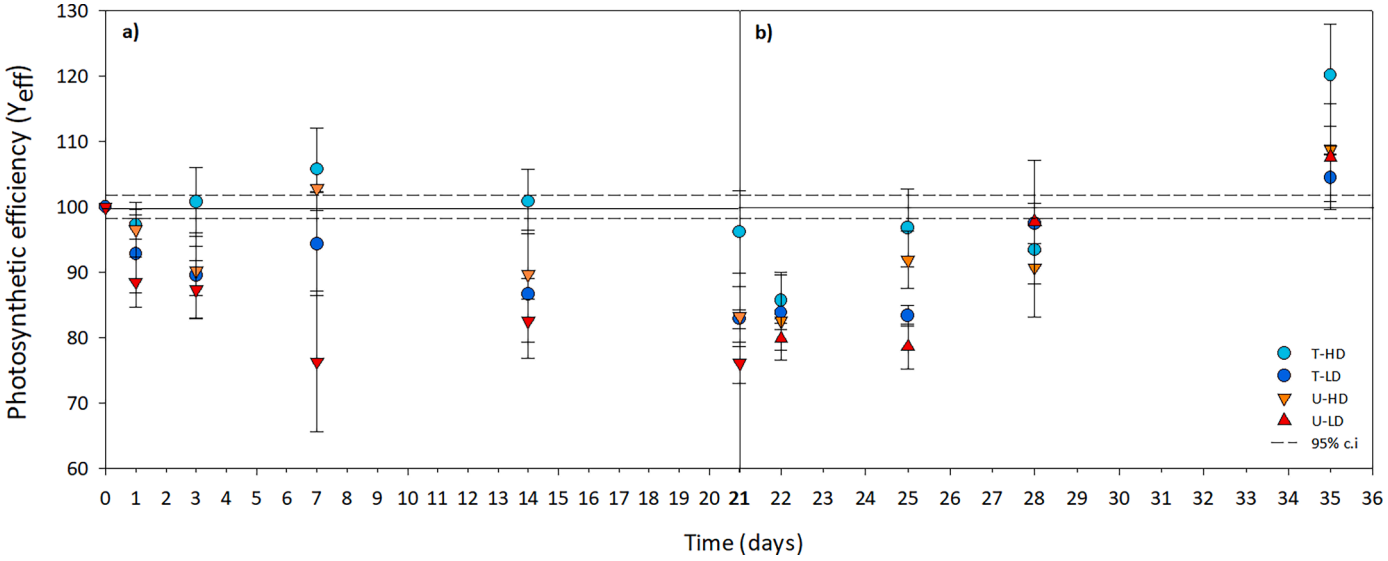

Fig. 2. Photosynthetic efficiency (Yeff) of the biofilm under the different treatments during the exposure (a) and recovery (b) periods in% variation from control (black line). Values are mean ± SD ($n = 3$). c.i: 95% confidence interval (dash line). Circles correspond to the treated and the triangles to the untreated effluents. Light blue and orange correspond to high dilution and dark blue and red to the low dilution scenario. T-HD: treated high dilution, T-LD: treated low dilution, U-HD: untreated high dilution, U-LD: untreated low dilution.

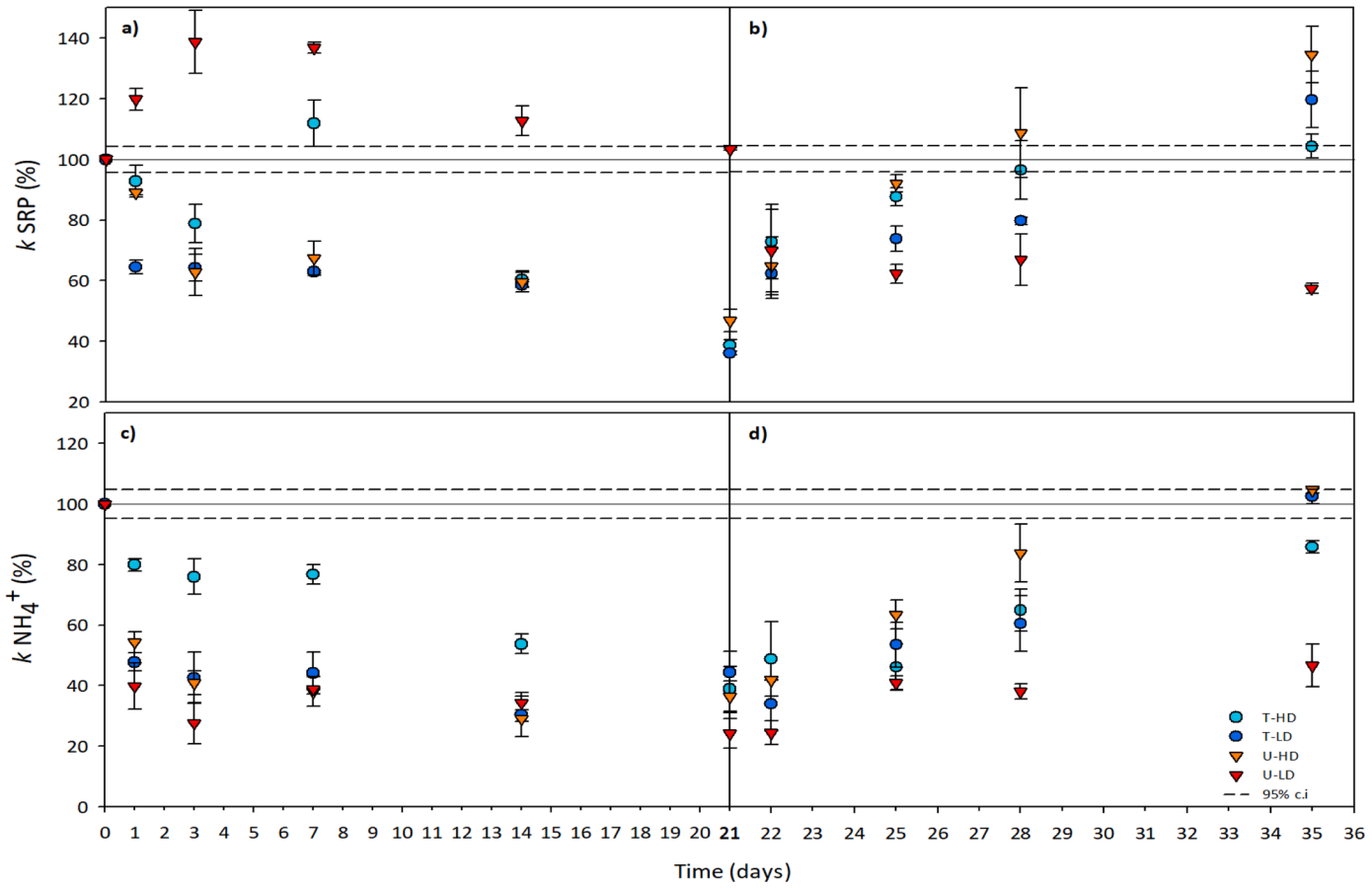

Fig. 3. SRP and NH_4^+ uptake (k) capacity of the biofilm communities under the different treatments during the exposure (a and c) and recovery (b and d) periods in% variation from control (black line). Values are mean ± SD ($n = 3$). c.i: 95% confidence interval (dash line). Circles correspond to the treated and the triangles to the untreated effluents. Light blue and orange correspond to high dilution and dark blue and red to the low dilution scenario. T-HD: treated high dilution, T-LD: treated low dilution, U-HD: untreated high dilution, U-LD: untreated low dilution.

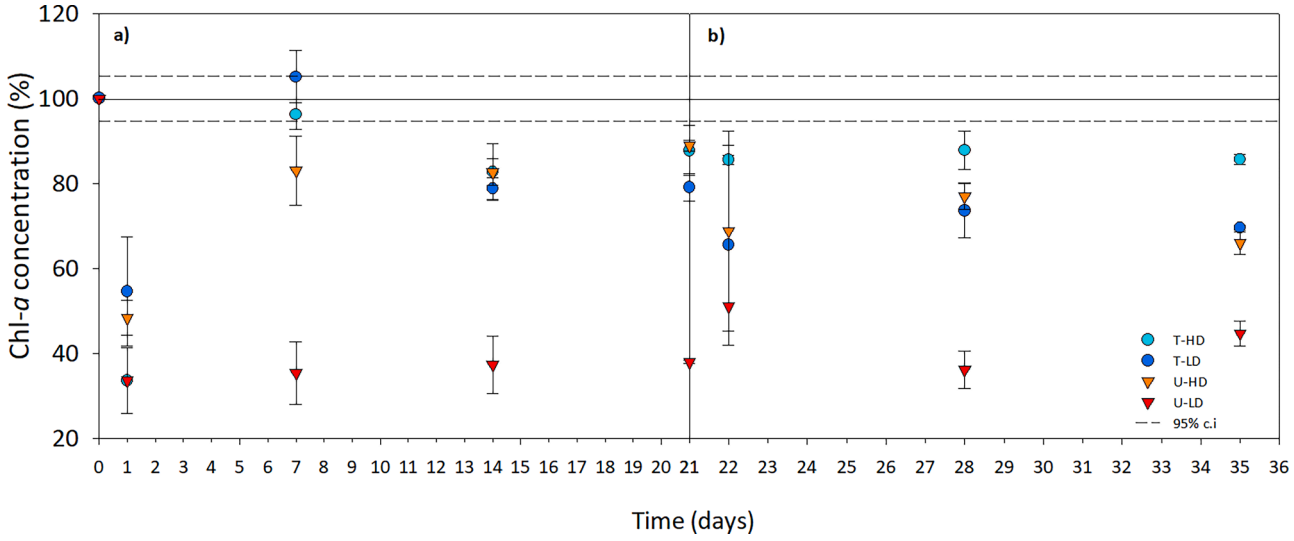

Fig. 4. Biofilm chlorophyll-*a* concentration under the different treatments during the exposure (a) and recovery (b) periods in% variation from control (black line). Values are mean ± SD ($n = 3$). c.i: 95% confidence interval (dash line). Circles correspond to the treated and the triangles to the untreated effluents. Light blue and orange correspond to high dilution and dark blue and red to the low dilution scenario. T-HD: treated high dilution, T-LD: treated low dilution, U-HD: untreated high dilution, U-LD: untreated low dilution.

way ANOVA, $F = 10.6$, $p < 0.001$), with U-LD significantly smaller than the rest of treatments at t21d (Tukey b test, $p < 0.05$). Furthermore, Zn accumulation in biofilm presented a negative correlation with the diatom GR (Pearson's correlation $r = -0.785$, $p < 0.001$) and cell size (Pearson's correlation $r = -0.794$, $p < 0.001$). In addition, a decrease on the diatom species richness after 3 days of exposure (t3d) was observed

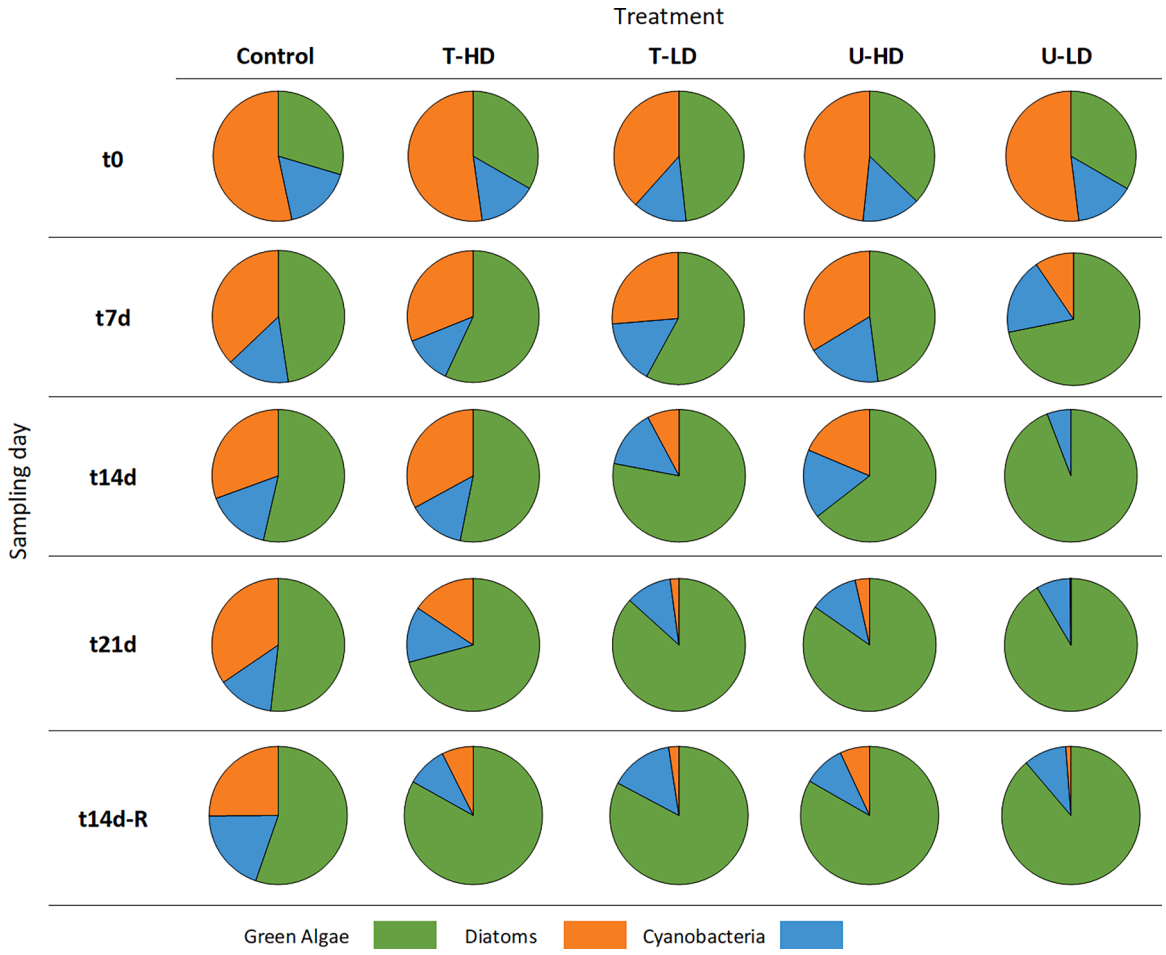

Fig. 5. Relative abundance (%) of each algal group conforming the photosynthetic community composition of the biofilm on each treatment before the exposure period (t0) during the exposure (t7, 14 and 21d) and recovery (t14d-R) periods ($n = 3$). The results present the mean values of three replicates of each treatment and sampling day. T-HD: treated high dilution, T-LD: treated low dilution, U-HD: untreated high dilution, U-LD: untreated low dilution.

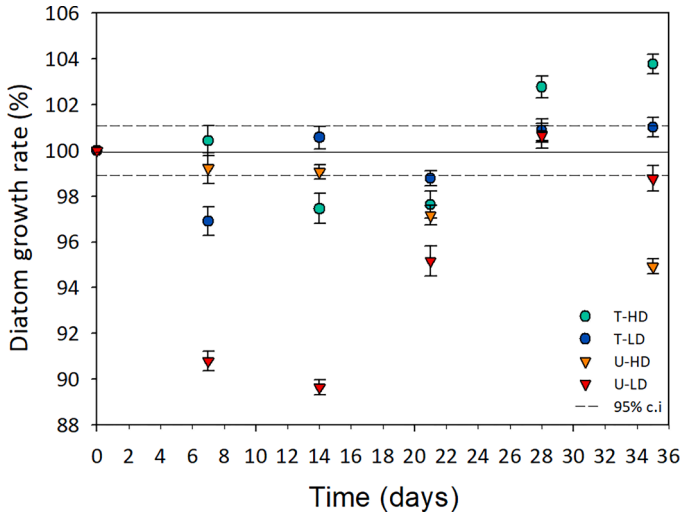

Fig. 6. Diatom growth rate (div day^{-1}; mean ± SD; $n = 3$) at each treatment, during the exposure and recovery periods in% variation from control (black line). c.i: 95% confidence interval (dash line). Circles correspond to the treated and the triangles to the untreated effluents. Light blue and orange correspond to high dilution and dark blue and red to the low dilution scenario. T-HD: treated high dilution, T-LD: treated low dilution, U-HD: untreated high dilution, U-LD: untreated low dilution.

and maintained during all the exposure period in all treatments (one-way ANOVA $F = 1.72$, $p < 0.001$) decreasing the number of identified species from 34 in the C to 16 in the U-LD. From the different samples collected, over 46 diatom taxa were identified at t21d, and significant differences were observed among the exposed diatom communities and the C (one-way ANOSIM, $R = 1$, $p = 0.008$, Fig. 7). In addition, Zn accumulation in the biofilm presented a negative correlation with the species richness of the diatom community (Pearson's correlation $r = -0.651$, $p = 0.009$).

Nevertheless, an increase in the diatom GR was observed in all treatments during the recovery period (one-way ANOVA, Treatment, $F = 89.2$, $p < 0.05$). The GR of those biofilms exposed to T-HD recovered, presenting significant higher rates than the C while T-LD did not present significant differences to the C. On the other hand, U-HD and U-LD presented long term effects by not recovering their GR and remained below the C (Fig. 6). However, diatom diversity did not recover under any treatment during the recovery period, and at t14d-R the number of identified species were 34 at C to 29, 21, 18 and 16 in biofilm exposed to T-HD, T-LD, U-HD, and U-LD, respectively. Additionally, the diatom species in exposed biofilms presented significantly smaller sizes than the C at t21d, ranging from 127 μm in the C to 32.3 μm in the U-LD; Figure S2). At the end of the recovery period, the diatom size did not recover compared to the C and smaller forms were still observed in exposed communities. However, at the end of the recovery period (t14d-R), a significant change in the species dominance was observed in all treatments with respect to the C. Specifically, an increase in *Navicula antonii* (Lange-Bertalot), which was the most abundant specie among all

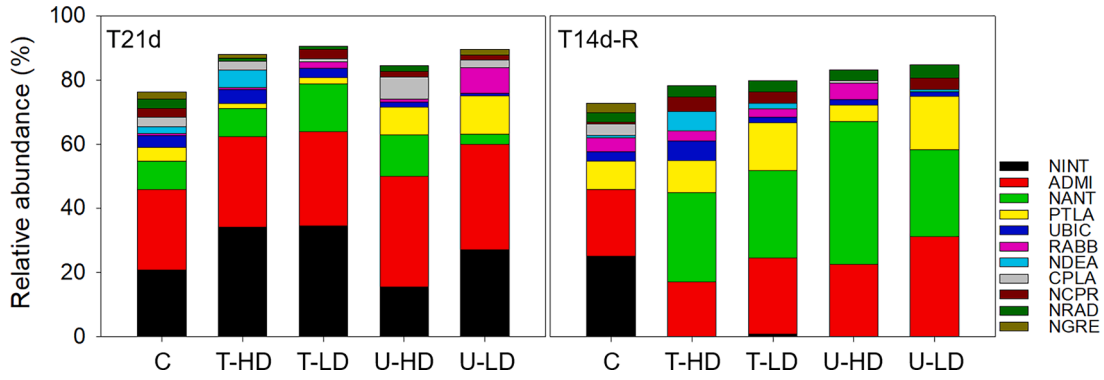

Fig. 7. Relative abundance (mean value, $n = 3$) of the ten major diatom species (>3%) within diatom communities collected in the artificial streams at the end of the exposure and recovery periods. Where *Nitzschia intermedia* (NINT), *Achnantidium minutissimum* (ADMI), *Navicula antonii* (NANT), *Plathonidium lanceolatum* Brébisson ex Kützing (PTLA), *Ulnaria biceps* Kützing (UBIC), *Rhoicosphenia abbreviata* C.Agardh (RABB), *Navicula dealpiniana* Lange-Bertalot (NDEA), *Cocconeis placentula* Ehrenberg (CPLA), *Navicula capitoradiata* H.Germain ex Gasse (NCPR), *Navicula radiosa* Kützing (NRAD), and *Navicula gregaria* Donkin (NGRE). 21d: 21 days after the exposure, 14-R: 14 days after the recovery. R and p values of the one-way ANOSIM being $R = 0.186$, $p < 0.001$ at t21d, and $R = 0.365$, $p < 0.001$ at t 14d-R.

exposed biofilms were observed, while *Nitzschia intermedia* (Hantzsch) almost disappeared (Fig. 7).

3.2.6. Metal accumulation in biofilm

Metal accumulation occurred in biofilm exposed to the mining effluents during the exposure period. Significant differences were observed in the accumulation of Zn (one-way ANOVA, $F = 93.2$, $p < 0.001$), Pb (one-way ANOVA, $F = 99.4$, $p < 0.001$) and Cd (one-way ANOVA, $F = 350$, $p < 0.001$) in the biofilm among treatments at the end of this period (t21d). These differences were especially evident in the biofilm exposed to U-LD, which presented 80, 40 and 2-fold more Zn, Pb and Cd accumulation than C biofilm, respectively (Fig. 8). In contrast, biofilm exposed to T-HD did not show significant differences in metal accumulation with respect to the C for any of the metals measured (Fig. 8). At t14d-R, still significant differences in the accumulation of Zn (one-way ANOVA, $F = 23.2$, $p < 0.001$), Pb (one-way ANOVA, $F = 4.97$, $p = 0.018$) and Cd (one-way ANOVA, $F = 30.2$, $p < 0.001$) among treatments and the C were observed, being especially evident in U-LD biofilms that accumulated 23, 37 and 1.3-fold more Zn, Pb and Cd, respectively, than the C (Fig. 8).

3.2.7. Threshold indicator taxa analysis (TITAN analysis)

TITAN analysis was applied to identify diatom indicator taxa and diatom community sensitivity thresholds to the pollution among the most abundant diatom taxa. The analysis was applied to the Zn and pH gradient since they showed the most significant response to the different exposures. Our results demonstrated that at t21d, the community-level change point where non-tolerant species decreased was at Zn concentration of 0.79 mg Zn L^{-1} and pH 6.72. Nevertheless, at the end of the recovery period (t14d-R), the decrease in this non-tolerant species was found at 0.01 mg Zn L^{-1} and pH 7.06 (Fig. 9). By contrast, the community-level change points for the tolerant community at t21d were calculated at 1.39 mg Zn L^{-1} and pH of 6.88, while at t14d-R the change points were found at 0.01 mg Zn L^{-1} and pH 7.09 (Fig. 9). Most of the positive responder taxa were associated with higher pH, and negative responder taxa were related to high Zn concentrations. Using TITAN, we found that only a subset of the diatom taxa (range: 2%–20% of the 46 taxa depending on the environmental variable considered) responded reliably to the two environmental variables.

3.3. Overall biofilm responses

The first axis of the PCA at t21d explains the 57.5% of the variance and was linked to the dilution factor (Fig. 10-A). Treatments U-LD and T-LD are separated from the other treatments and the C. This separation is mostly driven by higher metal accumulation and green algae abundance in LD treatments. Nevertheless, the C shows higher photosynthetic efficiency, nutrient uptake capacities, chl-*a*, and diatom abundance in the biofilm. The second axis of the PCA explains the 21.2% of the variance and it is driven by cyanobacteria abundance and the MI (Margalefs Index), separating the T and U of the LD scenarios.

On the other hand, the first axis of the second PCA at t14d-R (Fig. 10-B) explains the 39.8% of the variance separating again LD treatments from the other treatments. These treatments are characterised by higher metal accumulation, green algae, and cyanobacteria abundance. The second axis explains the 28.5% of the variance and it separates treatments T-LD and U-HD on the upper part of the PCA from the other treatments.

4. Discussion

In the present study different biofilm alterations were observed during a 21-day exposure period. These effects included altered photosynthetic efficiency, nutrient uptake rate, community composition, reduced diatom species richness and growth rate, and a decrease in the metal accumulation in biofilm communities exposed to both, treated and untreated mining effluent under the low diluted (LD) scenario. However, following a 14-day recovery period, the functionality of affected biofilms recovered except for those communities exposed to the untreated effluent under high diluted scenario (U-HD) treatment. Nevertheless, the community composition of biofilms exposed to all treatments remained altered after t14d-R.

4.1. Biofilm functional responses during the exposure period

A drastic decrease in the photosynthetic efficiency (Y_{eff}) was observed just after 24 h of exposure in T-LD, U-HD, and U-LD treatments. This effect has been previously described (A. Tlili et al., 2011; Bonet et al., 2014), and explained by metals mode of action compromising different photosynthetic paths of biofilm communities (Admiraal et al., 1999) such as the electron transport flow (Juneau et al., 2007). Comparable results were reported in biofilms exposed to 400 μg Zn L^{-1} under microcosm-controlled conditions (Corcoll et al., 2011) or under Zn concentrations of 4.25 mg Zn L^{-1}, in a previous study using a metal mining effluent from the same abandoned mine (Vendrell-Puigmitja et al., 2020). On the other hand, Gonçalves et al. (2018) indicated that changes in the diatom's metabolome occurred at 500 μg Zn L^{-1}.

In addition to the decrease in photosynthetic efficiency, the metal mining effluent caused a general and significant decrease in the capacity of exposed biofilm to take up phosphorus (SRP) and ammonium (NH_4^+) from the water column (except for U-LD for SRP). The exposure to heavy metals can affect the biofilm capacity to assimilate SRP and NH_4^+ (A.

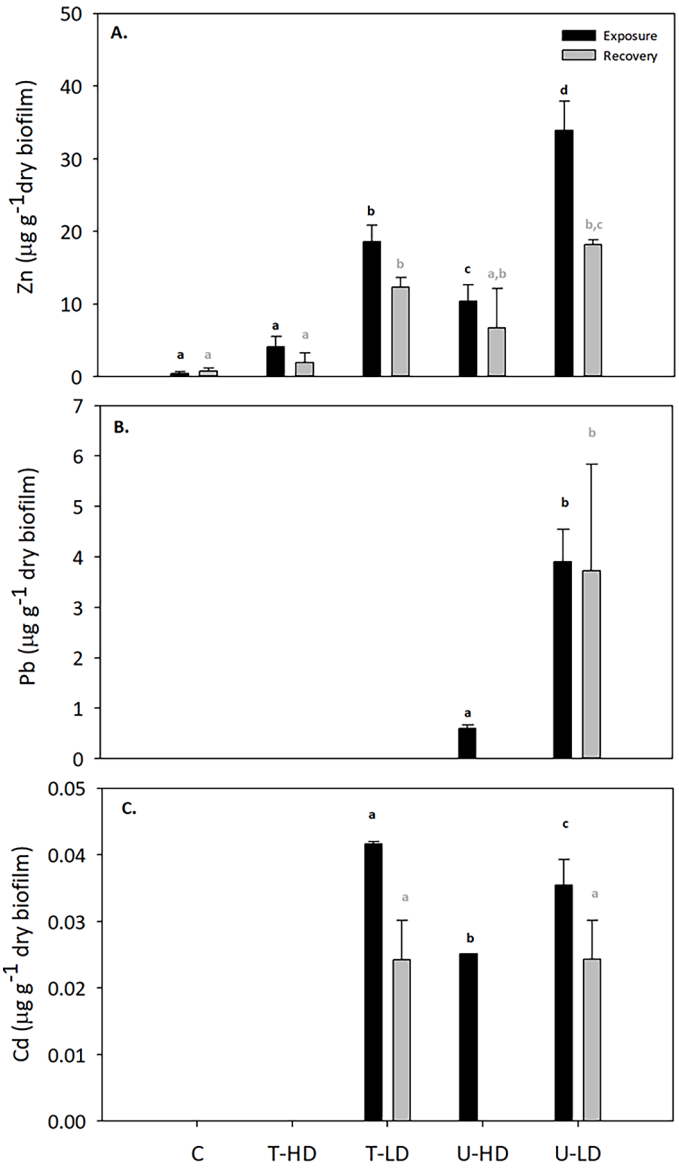

Fig. 8. Metal accumulation in biofilms (A. Zn accumulation; B. Pb accumulation; C. Cd accumulation) under the different treatments at the end of the exposure (after 21 days) and recovery (after 14 days of recovery) period. T-HD: treated high dilution, T-LD: treated low dilution, U-HD: untreated high dilution, U-LD: untreated low dilution. Mean ± SD (n = 3). The lower-case letters indicate significant differences ($p < 0.05$) between treatments at each time (t21d and t14d-R) after one-way ANOVA and Tukey b test.

Serra, 2009; Proia et al., 2017). Heavy metals could promote oxidative damage in the algal cells that might have reduced the nutrient uptake capacity of exposed biofilm communities (Sabater et al., 2007). In addition, the oxidative stress might have caused a change in the energy investment from nutrient uptake to antioxidant enzyme activities production as detoxification mechanisms (Morin et al., 2012; Bonet. 2013). This was also reported by Castro et al. (2015) and Tuulaikhuu et al. (2015) under stress generated by exposure to arsenic (As) concentrations of 130 µg L^{-1} and 37 µg L^{-1}, respectively. Furthermore, the nutrient uptake capacity of biofilm communities is influenced by the biofilm biomass (Guasch et al., 2003; Proia et al., 2017) which in this study decreased with the increase of the metal concentrations. In the highest metal concentration scenario (U-LD), the increase in the SRP uptake might have been caused by an abiotic removal of phosphorous promoted by the metal complexation with phosphate, such as $Zn_3(PO_4)_2$ and $Pb_5(PO_4)_3Cl$, leading to its precipitation (Zhu et al., 2016; Seshadri et al., 2017). In fact, in Lu et al. (2021) Zn precipitated with inorganic phosphate at Zn concentrations between 1 and 10 mg L^{-1}, a concentration that was exceeded in this study. This suggests that in the field, the discharge of the untreated mining effluents to the stream under low flow conditions can cause phosphate removal from the water column through precipitation. This could be an impediment for freshwater organisms to grow and develop since phosphorus is an essential nutrient playing indispensable roles in ATP synthesis and mineralization, among other processes (Vendrell-Puigmitja., 2021; Argudo et al., 2020; Corcoll et al., 2012; Rumschik et al., 2009). Long-term phosphorus deficiency can lead to a significant decrease in nitrogen removal efficiency (Zhang et al., 2020). In the field, natural streams affected by metal mining effluents could have a decrease in its self-depuration capacity (Hamdhani et al., 2020; Grizzetti et al., 2019; Castro et al., 2015; Bothwell 1988). On the other hand, phosphorus precipitation is reported to inhibit the biosynthesis of chl-*a* (Li et al., 2016). The biomass (i.e., chl-*a*) determines the effects of toxicants, thus with its reduction, diffusion of toxicants might increase (Sabater et al., 2002).

4.2. *Biofilm structural responses during the exposure period*

Regarding the changes in biomass (i.e., chl-*a*), our results showed a drastic decrease during the exposure period, on biofilms exposed to T-LD, U-HD and U-LD compared to the C From Zn concentrations in water of 0.19 mg·L^{-1}. Corcoll et al. (2011) reported similar results after long-term exposures to 400 µg Zn·L^{-1} in water. Paulsson et al. (2002) observed the same effects at Zn concentrations between 6 and 25 µg·L^{-1}. By contrast, Guasch et al. (2003), reported that Zn toxicity on biofilm was highly related to algal biomass thus the range of EC_{10} values based on photosynthesis tests was very extensive (455 – 65,000 µg Zn L^{-1}). Concerning Cd, in this study effects were observed even at concentrations below the detection limit. However, previous studies (Gold et al., 2003b; Morin et al., 2008) showed slight effects at 10 µg·L^{-1}, and a prominent reduction of the biofilm biomass after chronic exposure to 100 µg·L^{-1}. Similarly to the results with Cd, we could see effects in chl-*a* for Pb concentrations below the detection limit. Nevertheless, Fechner et al. (2010) observed effects at Pb concentrations around 50 mg·L^{-1}. The reduction in the chl-*a* could be related to the substitution of magnesium, the central atom of chlorophyll, by heavy metals leading to an inhibition of chlorophyll production (Baumann et al., 2009; Corcoll et al., 2011). The mentioned decrease might imply effects on the freshwater ecosystems due to their role in the uptake or retention of inorganic and organic nutrients (Fishcer et al., 2002; Romaní et al., 2004), also affecting the self-depuration processes, and transfer of energy to higher trophic levels (Corcoll et al., 2011).

On the other hand, a shift in the biofilm community composition was observed where green algae dominated the exposed biofilms community. In fact, green algae are known to be favoured after long-term exposure to Zn concentration (Ivorra et al., 2000; Corcoll et al., 2011 and Vendell-Puigmitja et al., 2020), and present high abundances in metal polluted aquatic environments (Das and Ramanujam, 2011). Different mechanisms could enable green algae to tolerate chemical stress caused by heavy metal concentrations such as a decrease in the number of binding sites at the cell surface, internal detoxifying mechanisms (Gold et al., 2003) or additional enzymatic activity provided by metals (Pawlik-Skowronska 2003). These mechanisms were described by Corcoll et al. (2012) and are related to Zn toxicity that may enhance the synthesis of antioxidants causing the activation of the xanthophyll cycle of green algae as protective mechanisms to avoid Zn toxicity.

Despite diatoms dominating (48.9 ± 3%) the biofilm community just before the exposure period started, this algal group drastically reduced its abundance during the exposure to T-LD, U-HD, and U-LD, whereas abundance remained similar to the control in T-HD, until the end of the exposure period (t21d). However, the diatom size, diversity, and growth rate decreased in all treatments, including the T-HD. The diatom community response varied along the Zn concentration and pH gradient and

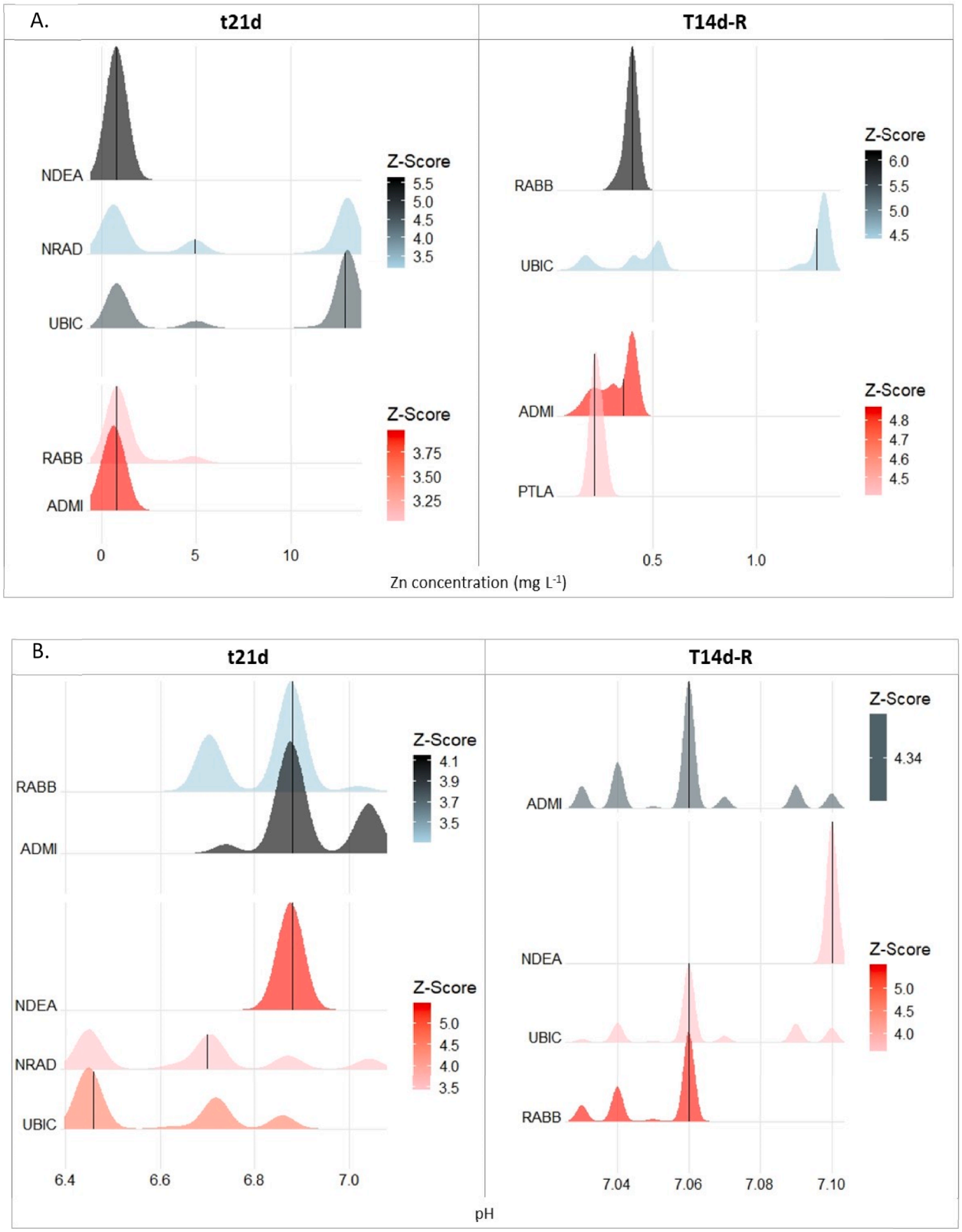

Fig. 9. Plot of sum z-scores for responding diatom taxa along the A. Zn and B. pH gradient. Steep slopes indicate major change points in abundance. Red corresponds to tolerant species (i.e., positive responders) that increased with the increasing Zn and pH values (z+), and in blue the non-tolerant species (i.e., negative responders) that decreased with the increase on pH and Zn (z-). 21d: 21 days after the exposure, 14-R: 14 days after the recovery.

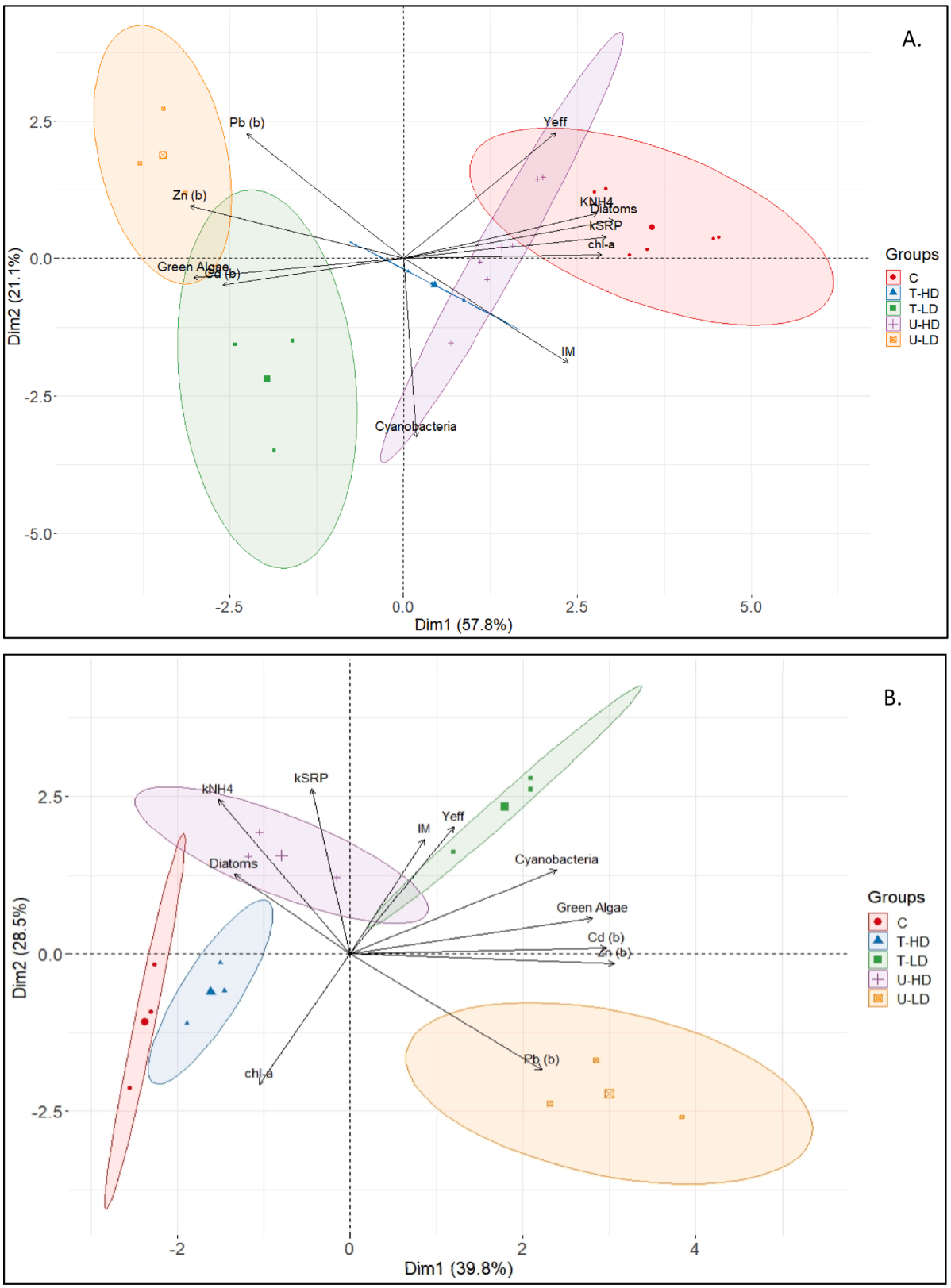

Fig. 10. Biplot of the principal component analysis (PCA), with data points identified by treatment. Vectors plotted to indicate the correlation scores between the structural and functional variables evaluated at the end of the exposure (A) and recovery period (B). chl-*a*, chlorophyll-a; KNH4, ammonium uptake rate; KSRP, soluble reactive phosphate uptake rate; IM, Margalef index; Yeff, photosynthetic efficiency; Zn, Pb and Cd(b), metal accumulation. The ellipses indicate 95% confidence around their centroids for treatment. C: control in red circles, T-HD: treated high diluted in blue triangles (in graph A appears as a line), T-LD: treated low diluted in green squares, U-HD: untreated high diluted in purple cross, U-LD: untreated low diluted in orange squares.

the concentrations from which diatom abundance decreased was 0.79 mg $Zn{\cdot}L^{-1}$ and pH 6.72. However, in a previous study performed in the same receiving stream (Frongoch stream), Vendrell-Puigmitja (2021) reported that the diatoms decreased at 1 mg Zn·L-1 and pH of 6.3. This might suggest that under field conditions, chronic exposures might promote adaptations to the pollution gradient (Blanck. 2002). In this case, the diatom species identified above these thresholds were described as tolerant (e.g., Morin et al., 2014; Cantonati et al., 2014; Lavoie et al., 2018) to metal concentration (Medley and Clements, 1998), and frequently reported in metal contaminated environments (Morin et al., 2012). Certainly, environmental factors such as the exposure to toxic agents (i.e., metals), determine the diatom composition by favouring tolerant species (Morin et al., 2012). On the other hand, diatom cell size and diversity decreased regardless of both treatment and dilution. In impacted sites, the decrease on the diatom cell size is related to the dominance of smaller growth forms (Sabater and Admiraal, 2005), since they are more effectively protected by the exopolysaccharide matrix and thus its survival is favoured under heavy metal pollution (Morin et al., 2012).

Furthermore, an increase in metal concentration in the biofilm was observed even when Cd and Pb were not detected in water. Biofilms have a large number of metal binding sites located in either mucopolysaccharides at the surface of cells or in the organic particles trapped by the biofilm. These substances can play a significant role in the sorption of dissolved metals from water column (Bere et al., 2012; Duong et al., 2008, 2010). The metals can slowly enter the cells by active metal transport into the intracellular pool, also called absorption or bio-uptake (A. Serra et al., 2009). The accumulation of metals by biofilm communities increases with larger exposure times (Collard and Matagne, 1994), and becomes toxic when intracellular metal is present at high concentration, exerting a negative influence on the biochemical mechanisms of the cells (Corcoll et al., 2012). The presence of metal ions can affect many aspects of biofilm communities including biomass, metabolic activity (e.g., photosynthesis), and extracellular polymeric substances (EPS) production (Tang et al., 2017), which play the most key role in biofilm protection to metal toxicity (Zhu et al., 2019).

4.3. Biofilm responses during the recovery period

During the recovery period, biofilm communities previously exposed to the mining effluent recovered the photosynthetic efficiency and algal biomass. Biofilm exposed to T-HD, T-LD and U-HD also recovered the nutrient uptake capacity during the transition to clean water conditions. This recovery might be caused by the increase in the number of cell transporters excreting accumulated metals in cells as a consequence of a detoxification mechanism acquired after the exposure period (Castro et al., 2015). This extrusion was evidenced by the presence of Zn in water during the recovery phase (Table 1). Contrarily, communities previously exposed to treatment U-LD did not recover the SRP and NH_4^+ uptake capacity, probably caused by the high metal accumulation still detected in these communities (Duong et al., 2009; Bere et al., 2011).

On the other hand, during the recovery period, green algae kept dominating communities previously exposed to treated and untreated effluents both under low and high diluted conditions, even though before the exposure period biofilm communities were dominated by diatoms. Zn contamination could have exerted pressure on diatom communities proportional to exposure level and biofilm age (A. Tlili et al., 2011), leading to a reduction in their ability to grow in competition to green algae. Nevertheless, the diatom cell size and the growth rate of exposed biofilm remained below the C at the end of the recovery period confirming a potential chronic (or long-term) effect of the mining effluent on this group of primary producers independently from treatment and dilution. The reduction in the cell size is attributed to an uncontrollable silica condensation induced by exposure to heavy metals (Su et al., 2018). Cell size is a key trait determining the ability of diatom species to recover after disturbance since smaller cells have typically higher growth rates and nutrient uptake rates compared to larger ones that confer greater resilience (Lange et al., 2016), which might have been the case of this study. Additionally, the diatom community composition of biofilm during the recovery period changed in comparison to the exposure period and the C. This shift in the diatom species dominance might be favoured by the decrease of species dominant in the exposure period (mainly *Nitzschia intermedia* Hantzsch) during the transition to clean conditions, which favoured the growth of metal adapted ones such as *Rhoicosphenia abbreviata* C.Agardh (Morin et al., 2012; Tolotti et al., 2019). Diatom composition changes are linked with the adaptation process to long-term Zn pollution (A. Tlili et al., 2011b). It is known that returning the adapted communities exposed to a pollutant to reference conditions may not be possible after crossing a critical threshold (Wolff et al., 2019). The latter suggest exposure to the metal mining effluent selects diatom species with a better capacity to regulate intracellular metal concentration by means of energy-dependent active transport systems (Castro et al., 2015). This might have favoured the growth and establishment of tolerant species, able to recover functional activity but not ensure structural recovery. Besides, adding new inoculum during the recovery period might have favoured the process where species physiologically affected by the metal exposure could be replaced by more active species (Lambert et al., 2012). This indicated that structural changes could be more prominent than the functional ones, specially under microcosm conditions, suggesting strong functional redundancy of the adapted community (A. Tlili et al., 2011; Tlili et al., 2016).

Differences observed in the community composition between treatments and the C might be explained by the duration of the recovery period. In this study, 14 days of recovery were simulated, and communities possibly were not able to recover, indicating that a longer recovery period would be needed. For instance, Rimet et al. (2005) reported that diatom-dominated biofilm transferred from a polluted to an unpolluted site needed 40 to 60 days to recover according to the trophic diatom index (TDI). On the other hand, Arini et al. (2012a) reported incomplete biofilm recovery after 56 days of exposure to water free of metals. Moreover, in this study the recovery of the biofilm community could have been affected by the lack of inoculum addition during the recovery period. Indeed, it was previously reported that the biofilm recovery was more pronounced when species immigration processes were possible (Ivorra et al., 1999; Morin et al., 2010). In this regard, Lambert et al. (2012) observed a full recovery after 28 days only when previously exposed communities were mixed with pristine communities, which favoured the diatom growth and green algae reduction. However, the retention of contaminants in the biofilm prevents complete removal of the stress even though it is no longer present in the bulk liquid phase (Ivorra et al., 1999), which might be the case of the most polluted scenario (U-LD).

5. Conclusions

Even though the application of the remediation technology achieved good metal removals, biofilm exposed to the treated effluents still presented higher metal accumulation compared to the C, and was also affected by the level of dilution. This highlights the need to assess the efficiency of the treatment technologies considering the effluent metal composition and concentration, and the dilution capacity of the receiving stream. In natural environments, the ecological impacts caused by treated mining effluents may depend on the flow conditions of the receiving stream. This flow variation could cause difficulties to accomplish within the Water Framework Directive (WFD) limits of metal content in stream waters . However, the dilution capacity of the receiving stream is not included in the legislation, and our study evidence that it is crucial to consider it to estimate the ecological impact of a mining effluent in water bodies. Overall, this study demonstrates that it is not enough to monitor and control the pollutants level of the discharging effluents, yet the hydrology and ecological characteristics of

the water system in which treated streams are discharging have to be considered to prevent continued impacts.

CRediT authorship contribution statement

Lidia Vendrell-Puigmitja: Writing – review & editing, Writing – original draft, Validation, Methodology, Investigation, Formal analysis, Data curation, Conceptualization. **Lluís Bertrans-Tubau:** Writing – review & editing, Investigation. **Maria Roca-Ayats:** Writing – review & editing, Methodology. **Laia Llenas:** Writing – review & editing, Supervision. **Lorenzo Proia:** Writing – review & editing, Validation, Supervision, Methodology. **Meritxell Abril:** Writing – review & editing, Writing – original draft, Validation, Supervision, Project administration, Methodology, Investigation, Data curation, Conceptualization.

Declaration of competing interest

The authors declare that they have no known competing financial interests or personal relationships that could have appeared to influence the work reported in this paper.

Data availability

Data will be made available on request.

Supplementary materials

Supplementary material associated with this article can be found, in the online version, at doi:10.1016/j.aquatox.2024.106843.

References

Admiraal, W., Blanck, H., Buckert-De Jong, M., Guasch, H., Ivorra, N., Lehmann, V., Sabater, S., 1999. Short-term toxicity of zinc to microbenthic algae and bacteria in a metal polluted stream. Water Res. 33 (9), 1989–1996.

Allan, J.D., Castillo, M.M., 2007. Stream Ecology: Structure and Function of Running Waters. Springer Science & Business Media.

APHA (American Public Health Association), 1992. Method 4500-NO3-. Nitrogen (Nitrate)*. Standard Methods for the Examination of Water and Wastewater, 18th ed. Washington, D.C.

Argudo, M., Gich, F., Bonet, B., Espinosa, C., Gutiérrez, M., Guasch, H., 2020. Responses of resident (DNA) and active (RNA) microbial communities in fluvial biofilms under different polluted scenarios. Chemosphere 242, 125108.

Arini, A., Feurtet-Mazel, A., Maury-Brachet, R., Pokrovsky, O.S., Coste, M., Delmas, F., 2012. Recovery potential of periphytic biofilms translocated in artificial streams after industrial contamination (Cd and Zn). Ecotoxicology. 21 (5), 1403–1414.

Battin, T.J., Besemer, K., Bengtsson, M.M., Romani, A.M., Packmann, A.I., 2016. The ecology and biogeochemistry of stream biofilms. Nature Rev. Microbiol. 14 (4), 251.

Baumann, H.A., Morrison, L., Stengel, D.B., 2009. Metal accumulation and toxicity measured by PAM—Chlorophyll fluorescence in seven species of marine macroalgae. Ecotoxicol. Environ. Saf. 72 (4), 1063–1075.

Bere, T., Chia, M.A., Tundisi, J.G., 2012. Effects of Cr III and Pb on the bioaccumulation and toxicity of Cd in tropical periphyton communities: implications of pulsed metal exposures. Environ. Pollut. 163, 184–191.

Blanck, H., 2002. A critical review of procedures and approaches used for assessing pollution-induced community tolerance (PICT) in biotic communities. Hum. Ecol. Risk Assessment 8 (5), 1003–1034.

Bonet, B., Corcoll, N., Acuña, V., Sigg, L., Behra, R., Guasch, H., 2013. Seasonal changes in antioxidant enzyme activities of freshwater biofilms in a metal polluted Mediterranean stream. Sci. Total Environ. 444, 60–72.

Bonet, B., Corcoll, N., Tlili, A., Morin, S., Guasch, H., 2014. Antioxidant enzyme activities in biofilms as biomarker of Zn pollution in a natural system: an active biomonitoring study. Ecotoxicol. Environ. Saf. 103, 82–90.

Bonnineau, C., Artigas, J., Chaumet, B., Dabrin, A., Faburé, J., Ferrari, B.J., Pesce, S., 2021. Role of biofilms in contaminant bioaccumulation and trophic transfer in aquatic ecosystems: current state of knowledge and future challenges. Rev. Environ. Contaminat. Toxicol. Vol. 253, 115–153.

Bonnineau, C., Bonet, B., Corcoll, N., Guasch, H., 2011. Catalase in fluvial biofilms: a comparison between different extraction methods and example of application in a metal-polluted river. Ecotoxicology. 20 (1), 293–303.

Byrne, P., Wood, P.J., Reid, I., 2012. The impairment of river systems by metal mine contamination: a review including remediation options. Crit. Rev. Environ. Sci. Technol. 42 (19), 2017–2077.

Cantonati, M., Angeli, N., Virtanen, L., Wojtal, A.Z., Gabrieli, J., Falasco, E., Smirnova, S., 2014. Achnanthidium minutissimum (Bacillariophyta) valve deformities as indicators of metal enrichment in diverse widely-distributed freshwater habitats. Sci. Total Environ. 475, 201–215.

Castro, M.C.R., Urrea, G., Guasch, H., 2015. Influence of the interaction between phosphate and arsenate on periphyton's growth and its nutrient uptake capacity. Sci. Total Environ. 503, 122–132.

Chand, V., Vanavana, I., 2022. Evaluation of Spirogyra sp. as a bioindicator of heavy metal pollution in a tropical aquatic environment. Pollution Research 41 (2), 445–450.

Clements, W.H., Vieira, N.K., Church, S.E., 2010. Quantifying restoration success and recovery in a metal-polluted stream: a 17-year assessment of physicochemical and biological responses. J. Appl. Ecol. 47 (4), 899–910.

Collard, J.M., Matagne, R.F., 1994. Cd2+ resistance in wild-type and mutant strains of Chlamydomonas reinhardtii. Environ. Exp. Bot. 34 (2), 235–244.

Corcoll, N., Bonet, B., Leira, M., Guasch, H., 2011. Chl-a fluorescence parameters as biomarkers of metal toxicity in fluvial biofilms: an experimental study. Hydrobiologia 673 (1), 119–136.

Corcoll, N., Bonet, B., Morin, S., Tlili, A., Leira, M., Guasch, H., 2012. The effect of metals on photosynthesis processes and diatom metrics of biofilm from a metal-contaminated river: a translocation experiment. Ecol. Indic. 18, 620–631.

Coste, M., Boutry, S., Tison-Rosebery, J., Delmas, F., 2009. Improvements of the Biological Diatom Index (BDI): description and efficiency of the new version (BDI-2006). Ecol. Indic. 9 (4), 621–650.

Das, M., Ramanujam, P., 2011. Metal content in water and in green filamentous algae Microspora quadrata hazen from coal mine impacted streams of Jaintia Hills District, Meghalaya, India. Int. J. Bot. 7 (2), 170–176.

Dufrêne, M., Legendre, P., 1997. Species assemblages and indicator species: the need for a flexible asymmetrical approach. Ecol. Monogr. 67 (3), 345–366.

Duong, T.T., Morin, S., Herlory, O., Feurtet-Mazel, A., Coste, M., Boudou, A., 2008. Seasonal effects of cadmium accumulation in periphytic diatom communities of freshwater biofilms. Aquat. Toxicol. 90 (1), 19–28.

Edwards, P., Williams, T., Stanley, P., 2016. Surface water management and encapsulation of mine waste to reduce water pollution from Frongoch Mine, Mid Wales. IMWA 546–553.

Fechner, L.C., Gourlay-Francé, C., Uher, E., Tusseau-Vuillemin, M.H., 2010. Adapting an enzymatic toxicity test to allow comparative evaluation of natural freshwater biofilms' tolerance to metals. Ecotoxicology. 19 (7), 1302–1311.

Fischer, H., Sachse, A., Steinberg, C.E., Pusch, M., 2002. Differential retention and utilization of dissolved organic carbon by bacteria in river sediments. Limnol. Oceanogr. 47 (6), 1702–1711.

Gold, C., Feurtet-Mazel, A., Coste, M., Boudou, A., 2003. Impacts of metals (Cd, Zn) on the development of periphytic diatom communities within outdoor artificial streams along a pollution gradient. Arch. Environ. Toxicol 44, 189–197.

Gonçalves, S., Kahlert, M., Almeida, S.F., Figueira, E., 2018. A freshwater diatom challenged by Zn: biochemical, physiological and metabolomic responses of Tabellaria flocculosa (Roth) Kützing. Environ. Pollut. 238, 959–971.

Grizzetti, B., Liquete, C., Pistocchi, A., Vigiak, O., Zulian, G., Bouraoui, F., Cardoso, A.C., 2019. Relationship between ecological condition and ecosystem services in European rivers, lakes and coastal waters. Sci. Total Environ. 671, 452–465.

Guasch, H., Admiraal, W., Sabater, S., 2003. Contrasting effects of organic and inorganic toxicants on freshwater periphyton. Aquat. Toxicol. 64 (2), 165–175.

Guasch, H., Paulsson, M., Sabater, S., 2002. Effect of copper on algal communities from oligotrophic calcareous streams 1. J. Phycol. 38 (2), 241–248.

Häder, D.P., Banaszak, A.T., Villafañe, V.E., Narvarte, M.A., González, R.A., Helbling, E. W., 2020. Anthropogenic pollution of aquatic ecosystems: Emerging problems with global implications. Science of the Total environment 713, 136586.

Hamdhani, H., Eppehimer, D.E., Bogan, M.T., 2020. Release of treated effluent into streams: a global review of ecological impacts with a consideration of its potential use for environmental flows. Freshw. Biol. 65 (9), 1657–1670.

Hong, Y.J., Liao, W., Yan, Z.F., Bai, Y.C., Feng, C.L., Xu, Z.X., Xu, D.Y., 2020. Progress in the research of the toxicity effect mechanisms of heavy metals on freshwater organisms and their water quality criteria in China. J. Chem. 2020.

Ivorra, N., Bremer, S., Guasch, H., Kraak, M.H., Admiraal, W., 2000. Differences in the sensitivity of benthic microalgae to Zn and Cd regarding biofilm development and exposure history. Environ. Toxicol. Chem.: Int. J. 19 (5), 1332–1339.

Ivorra, N., Hettelaar, J., Tubbing, G.M.J., Kraak, M.H.S., Sabater, S., Admiraal, W., 1999. Translocation of microbenthic algal assemblages used for in situ analysis of metal pollution in rivers. Arch. Environ. Contam. Toxicol. 37 (1), 19–28.

Jeffrey, S.T., Humphrey, G.F., 1975. New spectrophotometric equations for determining chlorophylls a, b, c1 and c2 in higher plants, algae and natural phytoplankton. Biochemie und physiologie der pflanzen 167 (2), 191–194.

Juneau, P., Qiu, B., Deblois, C.P., 2007. Use of chlorophyll fluorescence as a tool for determination of herbicide toxic effect. Toxicol. Environ. Chem. 89 (4), 609–625.

Kaplan, D., Christiaen, D., Malis-Arad, S., 1987. Binding of heavy metals by algal carbohydrates. Algal. Biotechnol. 179–187.

Kassambara, A., 2016. Factoextra: extract and visualize the results of multivariate data analyses. R package version 1.

Kossoff, D., Dubbin, W.E., Alfredsson, M., Edwards, S.J., Macklin, M.G., Hudson-Edwards, K.A., 2014. Mine tailings dams: characteristics, failure, environmental impacts, and remediation. Appl. Geochem. 51, 229–245.

Lambert, A.S., Morin, S., Artigas, J., Volat, B., Coquery, M., Neyra, M., Pesce, S., 2012. Structural and functional recovery of microbial biofilms after a decrease in copper exposure: influence of the presence of pristine communities. Aquat. Toxicol. 109, 118–126.

Lange, K., Townsend, C.R., Matthaei, C.D., 2016. A trait-based framework for stream algal communities. Ecol. Evol. 6 (1), 23–36.

Lange-Bertalot, H. and Metzeltin, D. (1996) Indicators of Oligotrophy - 800 Taxa Representative of Three Ecologically Distinct Lake Types, Carbonate Buffered - Oligodystrophic - Weakly Buffered Soft Water. Lange-Bertalot, H. (ed.), Iconographia Diatomologica. Annotated Diatom Micrographs. Vol. 2. Ecology, Diversity, Taxonomy. Koeltz Scientific Books. Königstein, Germany, 2:390 pp.
Lavoie, I., Morin, S., Laderriere, V., Fortin, C., 2018. Freshwater diatoms as indicators of combined long-term mining and urban stressors in Junction Creek (Ontario, Canada). Environments 5 (2), 30.
Lê, S., Josse, J., Husson, F., 2008. FactoMineR: an R package for multivariate analysis. J. Stat. Softw. 25, 1–18.
Leguay, S., Lavoie, I., Levy, J.L., Fortin, C., 2016. Using biofilms for monitoring metal contamination in lotic ecosystems: the protective effects of hardness and pH on metal bioaccumulation. Environ. Toxicol. Chem. 35 (6), 1489–1501.
Leira, M., Sabater, S., 2005. Diatom assemblages distribution in Catalan rivers, NE Spain, in relation to chemical and physiographical factors. Water Res. 39 (1), 73–82.
Li, S., Wang, C., Qin, H., Li, Y., Zheng, J., Peng, C., Li, D., 2016. Influence of phosphorus availability on the community structure and physiology of cultured biofilms. J. Environ. Sci. 42, 19–31.
Lu, X., Huang, Z., Liang, Z., Li, Z., Yang, J., Wang, Y., Wang, F., 2021. Co-precipitation of Cu and Zn in precipitation of struvite. Sci. Total Environ. 764, 144269.
Medley, C.N., Clements, W.H., 1998. Responses of diatom communities to heavy metals in streams: the influence of longitudinal variation. Ecol. Appl. 8 (3), 631–644.
Meylan, S., Behra, R., Sigg, L., 2003. Accumulation of copper and zinc in periphyton in response to dynamic variations of metal speciation in freshwater. Environ. Sci. Technol. 37 (22), 5204–5212.
Mohammad, A.W., Teow, Y.H., Ang, W.L., Chung, Y.T., Oatley-Radcliffe, D.L., Hilal, N., 2015. Nanofiltration membranes review: recent advances and future prospects. Desalination. 356, 226–254.
Morin, S., Coste, M., 2006. Metal-induced Shifts in the Morphology of Diatoms from the Riou Mort and Riou Viou Streams (South West France). Use of algae for monitoring rivers VI. Hungarian Algological Society, Hungary, Balatonfüred, pp. 91–106. Göd.
Morin, S., Corcoll, N., Bonet, B., Tlili, A., Guasch, H., 2014. Diatom responses to zinc contamination along a Mediterranean river. Plant Ecol. Evol. 147 (3), 325–332.
Morin, S., Cordonier, A., Lavoie, I., Arini, A., Blanco, S., Duong, T.T., Sabater, S., 2012. Consistency in diatom response to metal-contaminated environments. Emerging and Priority Pollutants in Rivers. Springer, Berlin, Heidelberg, pp. 117–146.
Morin, S., Duong, T.T., Dabrin, A., Coynel, A., Herlory, O., Baudrimont, M., Coste, M., 2008. Long-term survey of heavy-metal pollution, biofilm contamination and diatom community structure in the Riou Mort watershed, South-West France. Environ. Pollut. 151 (3), 532–542.
Morin, S., Proia, L., Ricart, M., Bonnineau, C., Geiszinger, A., Ricciardi, F., et al., 2010. Effects of a bactericide on the structure and survival of benthic diatom communities. Life Environ 60, 107–114.
Mullinger N. (2004) Review of environmental and ecological impacts of drainage from abandoned metal Minesin Wales. Environment Agency Wales report EATW/04/02.
Murphy, J.A.M.E.S., Riley, J.P., 1962. A modified single solution method for the determination of phosphate in natural waters. Anal. Chim. Acta 27, 31–36.
Pandey, L.K., Bergey, E.A., 2018. Metal toxicity and recovery response of riverine periphytic algae. Sci. Total Environ. 642, 1020–1031.
Park, J.H., Inam, E., Abdullah, M.H., Agustiyani, D., Duan, L., Hoang, T.T., Wirojanagud, W., 2011. Implications of rainfall variability for seasonality and climate-induced risks concerning surface water quality in East Asia. J. Hydrol. (Amst.) 400 (3–4), 323–332.
Paulsson, M., Månsson, V., Blanck, H., 2002. Effects of zinc on the phosphorus availability to periphyton communities from the river Göta Älv. Aquat. Toxicol. 56 (2), 103–113.
Pawlik-Skowrońska, B., 2003. When adapted to high zinc concentrations the periphytic green alga Stigeoclonium tenue produces high amounts of novel phytochelatin-related peptides. Aquat. Toxicol. 62 (2), 155–163.
Proia, L., Romaní, A., Sabater, S., 2017. Biofilm phosphorus uptake capacity as a tool for the assessment of pollutant effects in river ecosystems. Ecotoxicology. 26 (2), 271–282.
Reardon, J., Foreman, J.A., Searcy, R.L., 1966. New reactants for the colorimetric determination of ammonia. Clinica Chimica Acta 14, 403–405.
Rimet, F., Cauchie, H.M., Hoffmann, L., Ector, L., 2005. Response of diatom indices to simulated water quality improvements in a river. J. Appl. Phycol. 17 (2), 119–128.
Romaní, A.M., Giorgi, A., Acuna, V., Sabater, S., 2004. The influence of substratum type and nutrient supply on biofilm organic matter utilization in streams. Limnol. Oceanogr. 49 (5), 1713–1721.
Rumschik, S.M., Nydegger, I., Zhao, J., Kay, A.R., 2009. The interplay between inorganic phosphate and amino acids determines zinc solubility in brain slices. J. Neurochem. 108 (5), 1300–1308.
Sabater, S., Guasch, H., Ricart, M., Romaní, A., Vidal, G., Klünder, C., Schmitt-Jansen, M., 2007. Monitoring the effect of chemicals on biological communities. The biofilm as an interface. Anal. Bioanal. Chem. 387, 1425–1434.
Sabater, S., Admiraal, W., 2005. Periphyton as biological indicators in managed aquatic ecosystems. Periphyton: Ecol. Expl. Manag. 159–177.
Sabater, S., Guasch, H., Romaní, A., Muñoz, I., 2002. The effect of biological factors on the efficiency of river biofilms in improving water quality. Hydrobiologia 469 (1–3), 149–156.
Serra Gasa, A., 2009. Fate and Effects of Copper in Fluvial Ecosystems: The Role of Periphyton. Universitat de Girona.
Serra, A., Corcoll, N., Guasch, H., 2009. Copper accumulation and toxicity in fluvial periphyton: the influence of exposure history. Chemosphere 74 (5), 633–641.
Seshadri, B., Bolan, N.S., Choppala, G., Kunhikrishnan, A., Sanderson, P., Wang, H., Kim, G., 2017. Potential value of phosphate compounds in enhancing immobilization and reducing bioavailability of mixed heavy metal contaminants in shooting range soil. Chemosphere 184, 197–206.
Skousen, J.G., Ziemkiewicz, P.F., McDonald, L.M., 2019. Acid mine drainage formation, control and treatment: approaches and strategies. Extr. Ind. Soc. 6 (1), 241–249.
Su, Y., Lundholm, N., Ellegaard, M., 2018. Effects of abiotic factors on the nanostructure of diatom frustules—Ranges and variability. Appl. Microbiol. Biotechnol. 102, 5889–5899.
Sultana, J., Tibby, J., Recknagel, F., Maxwell, S., Goonan, P., 2020. Comparison of two commonly used methods for identifying water quality thresholds in freshwater ecosystems using field and synthetic data. Sci. Total Environ. 724, 137999.
... & Tang, J., Zhu, N., Zhu, Y., Liu, J., Wu, C., Kerr, P., Lam, P.K., 2017. Responses of periphyton to Fe2O3 nanoparticles: a physiological and ecological basis for defending nanotoxicity. Environ. Sci. Technol. 51 (18), 10797–10805.
Tchounwou, P.B., Yedjou, C.G., Patlolla, A.K., Sutton, D.J., 2012. Heavy metal toxicity and the environment. Mol. Clin. Environ. Toxicol. 133–164.
Tlili, A., Berard, A., Blanck, H., Bouchez, A., Cássio, F., Eriksson, K.M., Behra, R., 2016. Pollution-induced community tolerance (PICT): towards an ecologically relevant risk assessment of chemicals in aquatic systems. Freshw. Biol. 61 (12), 2141–2151.
Tlili, A., Corcoll, N., Bonet, B., Morin, S., Montuelle, B., Bérard, A., Guasch, H., 2011a. In situ spatio-temporal changes in pollution-induced community tolerance to zinc in autotrophic and heterotrophic biofilm communities. Ecotoxicology. 20, 1823–1839.
Tlili, A., Montuelle, B., Triquet, C.A., Rainbow, P.S., & Roméo, M. (2011). Microbial pollution-induced community tolerance. 85-108.
Tolotti, R., Consani, S., Carbone, C., Vagge, G., Capello, M., Cutroneo, L., 2019. Benthic diatom community response to metal contamination from an abandoned Cu mine: case study of the Gromolo Torrent (Italy). J. Environ. Sci. 75, 233–246.
Tripathi, A., Ranjan, M.R., 2015. Heavy metal removal from wastewater using low cost adsorbents. J. Bioremed. Biodegr. 6 (6), 1–5.
Tuulaikhuu, B.A., Romaní, A.M., Guasch, H., 2015. Arsenic toxicity effects on microbial communities and nutrient cycling in indoor experimental channels mimicking a fluvial system. Aquat. Toxicol. 166, 72–82.
Vendrell Puigmitjà, L. (2021). Assessment of the ecological impact of metal and salts mining effluents on freshwater bodies.
Vendrell-Puigmitja, L., Abril, M., Proia, L., Angona, C.E., Ricart, M., Oatley-Radcliffe, D. L., Llenas, L., 2020. Assessing the effects of metal mining effluents on freshwater ecosystems using biofilm as an ecological indicator: comparison between nanofiltration and nanofiltration with electrocoagulation treatment technologies. Ecol. Indic. 113, 106213.
Vendrell-Puigmitja, L., Proia, L., Espinosa, C., Barral-Fraga, L., Cañedo-Argüelles, M., Osorio, V., Abril, M., 2022. Hypersaline mining effluents affect the structure and function of stream biofilm. Sci. Total Environ. 843, 156966.
Wickham, H., 2016. ggplot2: Elegant Graphics For Data Analysis. Springer-Verlag, New York. ISBN 978-3-319-24277-4.
Wolff, B.A., Duggan, S.B., Clements, W.H., 2019. Resilience and regime shifts: do novel communities impede ecological recovery in a historically metal-contaminated stream? J. Appl. Ecol. 56 (12), 2698–2709.
Wu, Y., 2016. Periphyton: Functions and Application in Environmental Remediation. Elsevier.
Ylla, I., Borrego, C., Romaní, A.M., Sabater, S., 2009. Availability of glucose and light modulates the structure and function of a microbial biofilm. FEMS Microbiol. Ecol. 69 (1), 27–42.
Younger, P.L., Wolkersdorfer, C., 2004. Mining impacts on the freshwater environment: technical and managerial guidelines for catchment scale management. Mine Water. Environ. 23, s2.
Younger, P.L., Amezaga, J., Baresel, C., Destouni, G., Gren, I., Hannerz, F., 2003. Mining impacts on the fresh water environment: technical and managerial guidelines for catchment scale management. Environ 23, s2–s80.
Zhang, X., Li, B., Deng, J., Qin, B., Wells, M., Tefsen, B., 2020. Advances in freshwater risk assessment: improved accuracy of dissolved organic matter-metal speciation prediction and rapid biological validation. Ecotoxicol. Environ. Saf. 202, 110848.
Zhu, G., Wang, Q., Yin, J., Li, Z., Zhang, P., Ren, B., Wan, P., 2016. Toward a better understanding of coagulation for dissolved organic nitrogen using polymeric zinc-iron-phosphate coagulant. Water Res. 100, 201–210.
Zhu, N., Wang, S., Tang, C., Duan, P., Yao, L., Tang, J., Wu, Y., 2019. Protection mechanisms of periphytic biofilm to photocatalytic nanoparticle exposure. Environ. Sci. Technol. 53 (3), 1585–1594.